The MIX domain is required for T6SS-mediated effector secretion

Chaya Mushka Fridman[1,#], Biswanath Jana[1,#], Rotem Ben-Yaakov[1], Eran Bosis[2], & Dor Salomon[1,*]

[1] Department of Clinical Microbiology and Immunology, Sackler Faculty of Medicine, Tel Aviv University, Tel Aviv, Israel

[2] Department of Biotechnology Engineering, ORT Braude College of Engineering, Karmiel, Israel

[#] These authors contributed equally to this work

* Corresponding author. Tel: +972 3 6408583; E-mail: dorsalomon@mail.tau.ac.il

ABSTRACT

Bacteria use diverse classes of secreted polymorphic toxins to outcompete bacterial rivals. The MIX domain defines a widespread class of polymorphic type VI secretion system (T6SS) effectors, many of which are horizontally shared. Although several MIX-effectors have been investigated, the role of the MIX domain and the activity of many fused toxin domains remain unknown. Here, we use the *Vibrio parahaemolyticus* MIX-effector VPA1263 to demonstrate that MIX is necessary for T6SS-mediated secretion; however, we find that it is dispensable for interaction with the secreted T6SS tail tube component, VgrG. We also identify a C-terminal HNH nuclease toxin domain in VPA1263, and we demonstrate that it functions as a DNase during interbacterial competition. Finally, we identify variants of the genomic island containing *vpa1263* in various vibrios, each carrying a different cargo of antibacterial T6SS effectors or anti-phage defense systems. We propose that these genomic islands are hotspots for bacterial defensive weapons.

Keywords: polymorphic toxin, DNase, anti-phage, genomic island, competition

INTRODUCTION

Bacterial polymorphic toxins are modular proteins delivered by diverse secretion systems to mediate antibacterial or anti-eukaryotic activities (Jamet & Nassif, 2015; Zhang *et al*, 2012). They often share an N-terminal domain fused to diverse C-terminal toxin domains. The N-terminal domain, which can be used to classify these toxins, may determine which secretion system the effectors will be secreted through, e.g., the type V, VI, or VII secretion systems (T5/6/7SS, respectively) (Salomon *et al*, 2014a; Jamet & Nassif, 2015; Ruhe *et al*, 2020; Whitney *et al*, 2017; Aoki *et al*, 2010).

Many polymorphic toxins are secreted via T6SS, a contractile injection system widespread in Gram-negative bacteria (Pukatzki *et al*, 2006; Boyer *et al*, 2009). The toxins, called effectors, decorate a tail tube structure comprising Hcp, VgrG, and PAAR repeat-containing proteins (Silverman *et al*, 2013; Hachani *et al*, 2014; Burkinshaw *et al*, 2018); the tail tube is propelled outside of the cell by a contracting sheath structure that engulfs it (Basler *et al*, 2012). Effectors can be either specialized – tail tube proteins containing additional toxin domains at their C-termini – or cargo effectors, which are proteins that non-covalently bind to the tail tube, with or without the aid of an adaptor protein or a co-effector (Jana & Salomon, 2019; Jurėnas & Journet, 2021; Unterweger *et al*, 2015; Liang *et al*, 2015; Bondage *et al*, 2016; Alcoforado Diniz & Coulthurst, 2015; Cianfanelli *et al*, 2016; Dar *et al*, 2021). To date, three classes of polymorphic T6SS cargo effectors containing MIX (Salomon *et al*, 2014a), FIX (Jana *et al*, 2019), or Rhs (Koskiniemi *et al*, 2013) domains have been characterized; the Rhs domain is not restricted to T6SS effectors (Koskiniemi *et al*, 2013).

Proteins belonging to the MIX-effector class are secreted via T6SS (Salomon *et al*, 2014a; Miyata *et al*, 2011; Salomon *et al*, 2015; Ray *et al*, 2017). They contain a predominantly N-terminal MIX domain fused to known or predicted anti-eukaryotic or antibacterial C-terminal toxin domains; the latter precede a gene encoding a cognate immunity protein that prevents self or kin-intoxication (Ruhe *et al*, 2020; Hood *et al*, 2010; Russell *et al*, 2012). MIX domains can be divided into five clans that differ in their sequence conservation (Salomon *et al*, 2014a; Dar *et al*, 2018). Notably, members of the MIX V clan are common in bacteria of the *Vibrionaceae* family (Dar *et al*, 2018; Salomon *et al*, 2014a) and were suggested to be horizontally shared via mobile genetic elements (Salomon *et al*, 2015). MIX-effectors were reported to often co-occur with VgrG in genome neighborhoods (Salomon *et al*, 2014a). Although this observation hints at the possibility that MIX-effectors use VgrG as their point of contact on the T6SS tail tube, this hypothesis remains to be experimentally tested. Furthermore, it remains unknown whether MIX plays a role in T6SS-mediated secretion.

In previous work, we identified the MIX-effector VPA1263 as an antibacterial effector secreted by *V. parahaemolyticus* RIMD 2210633 T6SS1, and its downstream encoded Vti2 as the cognate immunity protein (Salomon *et al*, 2014a) (**Fig. 1A**). VPA1263 belongs to the MIX V clan. It is encoded on *V. parahaemolyticus* island-6 (VpaI-6), a predicted mobile genomic island that is present in a subset of *V. parahaemolyticus* genomes (Hurley *et al*, 2006). In this work, we aimed to decipher the toxic activity used by VPA1263 to intoxicate competitors, to determine VPA1263's secretion mechanism, and to reveal the possible role of the MIX domain in the secretion process; we also investigated the genomic island carrying *vpa1263*. We found that VPA1263 contains a C-terminal toxin domain belonging to the HNH nuclease superfamily, and showed that this domain functions as a DNase. Furthermore, we found that the MIX domain is required for secretion of VPA1263 via the T6SS, even though it is not required for interaction between VPA1263 and the T6SS tail tube component, VgrG. These results provide the first experimental validation of the hypothesis that MIX domains play a role in T6SS effector secretion. Moreover, they indicate that binding to a tail tube component is not sufficient to ensure T6SS-mediated delivery. We also found that in addition to VPA1263, VpaI-6 encodes an anti-phage defense system. Analysis of genomic islands homologous to VpaI-6 in other vibrios revealed a polymorphic cargo of anti-phage defense systems and antibacterial T6SS effectors.

RESULTS

VPA1263 contains a C-terminal HNH nuclease-like toxin domain

Analysis of the amino acid sequence of VPA1263 using the NCBI conserved domain database (Marchler-Bauer *et al*, 2007) revealed three known domains: a MIX domain (Salomon *et al*, 2014a), followed by a peptidoglycan-binding LysM domain (Buist *et al*, 2008), and a Pyocin_S domain (Michel-Briand & Baysse, 2002) (**Fig. 1B**). Hidden Markov modeling using HHPred (Zimmermann *et al*, 2018) revealed another region at the C-terminus of VPA1263 (amino acids 737-869) that is similar to the toxin domain found in members of the HNH nuclease superfamily, such as antibacterial S-type pyocins and colicins (Saravanan *et al*, 2004; Sano *et al*, 1993; Chak *et al*, 1991; Landthaler *et al*, 2004; Stoddard, 2005; Kala *et al*, 2014). An iterative search using a hidden Markov Model profile against the UniProt protein database indicated that the Pyocin_S and putative HNH nuclease domains located at the C-terminus of VPA1263 are also found together at the C-termini of other T6SS effectors containing the N-terminal PAAR, Hcp, or VgrG domains (**Supplementary Fig. S1A**); they were also found together in colicins such as colicin E9 and E7, although sometimes they were separated by a receptor binding domain. Interestingly, a similar HNH nuclease-like domain was also found in effectors containing N-terminal domains such as LXG (Whitney *et al*, 2017) and WXG100 (Poulsen *et al*, 2014), which are associated with T7SS but without an accompanying Pyocin_S domain. A conservation logo generated by aligning the amino acid sequences of the VPA1263 C-terminal domain (737-869) and homologous domains found in known or predicted secreted toxins confirmed the presence of a conserved His-Gln-His motif (Klein *et al*, 2016) (**Supplementary Fig. S1B**). These results led us to hypothesize that VPA1263 contains a C-terminal HNH nuclease domain that can mediate its antibacterial toxicity.

To determine the minimal region sufficient for VPA1263-mediated antibacterial toxicity, we ectopically expressed VPA1263 or its truncated versions (**Fig. 1B**) in *E. coli*. As shown in **Fig. 1C**, the C-terminal end, corresponding to the predicted HNH nuclease domain (amino acids 737-869; VPA1263$^{737\text{-}869}$), was necessary and sufficient to intoxicate *E. coli*. Notably, the expression of all VPA1263 versions, except for the toxic VPA1263$^{737\text{-}869}$, was detected in immunoblots (**Supplementary Fig. S2A**). Co-expression of the cognate immunity protein, Vti2 (Salomon *et al*, 2014a), rescued *E. coli* from the toxicity mediated by either the full-length VPA1263 or the C-terminal HNH nuclease domain (**Fig. 1D**), confirming that the toxicity mediated by the C-terminal HNH nuclease domain resulted from the same activity that is used by the full-length VPA1263. In addition, replacing the conserved histidine 837 with alanine (VPA1263^{H837A} or VPA1263$^{547\text{-}869/H837A}$) abrogated VPA1263-mediated toxicity (**Fig. 1E**), further supporting the role of the HNH nuclease domain in VPA1263-mediated antibacterial toxicity. Notably, the expression of the mutated proteins was confirmed in immunoblots (**Supplementary Fig. S2B**). Taken together, our results suggest that VPA1263 exerts its antibacterial toxicity via a C-terminal HNH nuclease domain.

VPA1263 is a DNase

Since HNH nucleases target DNA, we hypothesized that VPA1263 is a DNase. To test this hypothesis, we first set out to determine whether the C-terminal domain of VPA1263 can cleave DNA in vitro and in vivo. Since we were unable to purify the minimal toxin domain (amino acids 737-869), possibly due to low expression levels, we purified a truncated version encompassing both the C-terminal Pyocin_S and HNH nuclease domains (amino acids 547-869) (**Supplementary Fig. S3A**). As expected, this toxic region (VPA1263$^{547\text{-}869}$) was sufficient to cleave purified *E. coli* genomic DNA in vitro in the presence of $MgCl_2$, similar to DNase I, which was used as a control (**Fig. 2A**). In contrast, a mutated version, in which histidine 837 was replaced with alanine (VPA1263$^{547\text{-}869/H837A}$), did not cleave the DNA. Furthermore, we were only able to isolate small amounts of genomic DNA from *E. coli* cultures

expressing an arabinose-inducible VPA1263$^{547\text{-}869}$ or the *Bacillus cereus* DNase, BC3021 (PoNe^{BC}; (Jana *et al*, 2019)) (**Fig. 2B**), indicating that VPA1263 also cleaves DNA in vivo.

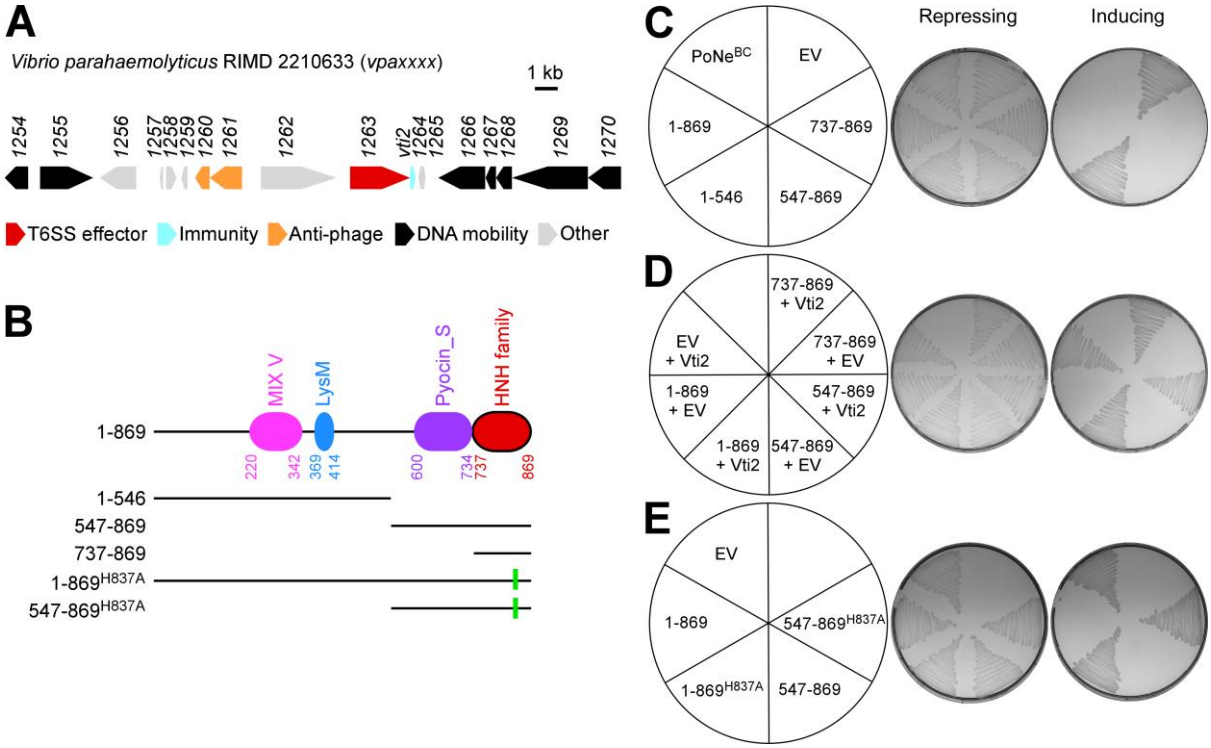

Figure 1. A C-terminal domain mediates VPA1263's antibacterial toxicity. (A) The *vpa1263* gene neighborhood (genome accession number BA000032.2). Genes are denoted by arrows indicating the direction of transcription. Locus tags (*vpaxxxx*) and unannotated gene names (i.e., *vti2*) are shown above. **(B)** Schematic representation of the domains identified in VPA1263 and of truncated and mutated variants examined in this figure. Green rectangles denote the position of the H837A mutation. **(C-E)** Toxicity of C-terminal Myc-His-tagged VPA1263 variants expressed from an arabinose-inducible expression plasmid in *E. coli* MG1655 streaked onto repressing (glucose) or inducing (arabinose) agar plates. In **D**, a second arabinose-inducible plasmid was used to co-express Vti2. EV, empty plasmid; PoNe^{BC}, a PoNe domain-containing DNase from *Bacillus cereus* (BC3021). The results shown represent at least three independent experiments.

Next, we set out to determine whether VPA1263 targets prey DNA during T6SS-mediated bacterial competition. To this end, we used fluorescence microscopy to visualize the DNA in bacterial cultures after T6SS-mediated self-competition. We competed a *V. parahaemolyticus* prey strain that constitutively expresses a green fluorescent protein (GFP) in which we deleted *vpa1263* and *vti2* (to specifically sensitize it to VPA1263-mediated toxicity) against attacker strains with a constitutively active T6SS1 (Salomon *et al*, 2014b), with or without a deletion in *vpa1263* (Δ*hns*/Δ*vpa1263* and Δ*hns*, respectively). Notably, these attacker strains exhibited similar growth rates (**Supplementary Fig. S3B**), and the Δ*hns*/Δ*vpa1263* strain retained the ability to intoxicate *Vibrio natriegens* prey in competition, indicating that its T6SS1 remained functional even though this attacker strain was unable to intoxicate a Δ*vpa1263-vti2* prey strain (**Supplementary Fig. S3C**). As shown in **Fig. 2C,D**, VPA1263-sensitive, GFP-expressing prey cells devoid of DNA or containing DNA foci (visualized with the fluorescent DNA dye, Hoechst) were only detected after competition against the VPA1263^{+} attacker strain (Δ*hns*). Taken together, these results support the notion that VPA1263 is a T6SS1 DNase effector.

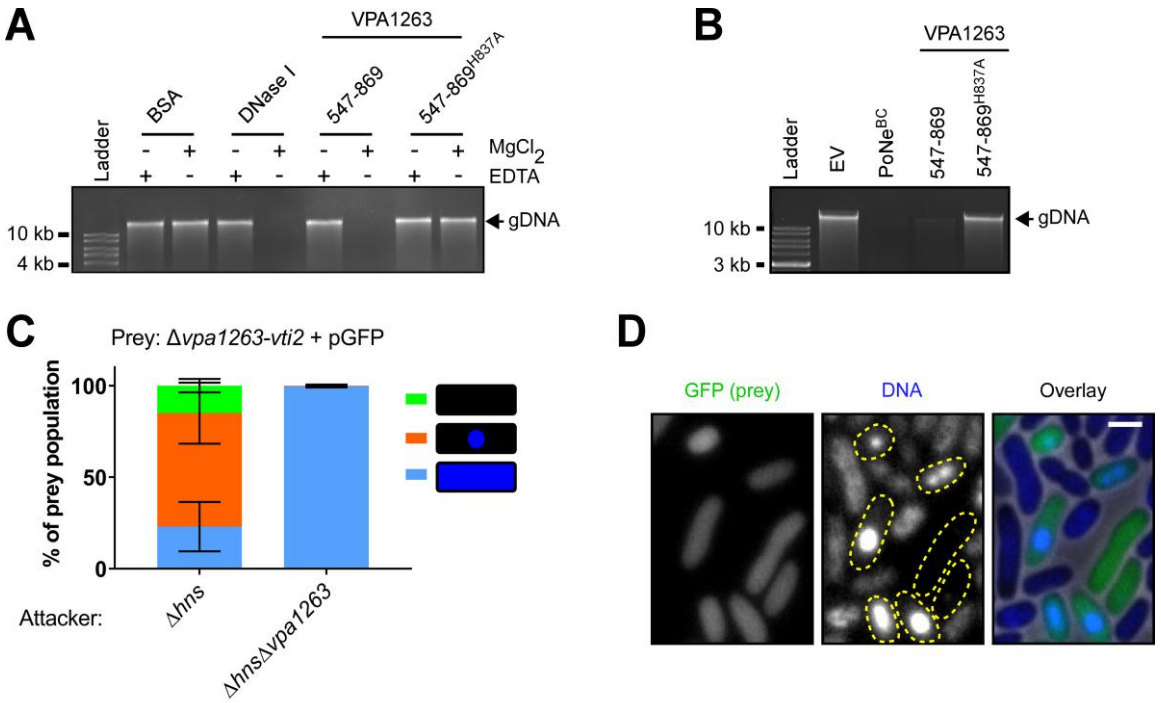

Figure 2. VPA1263 is a DNase. (A) In vitro DNase activity. Purified *E. coli* genomic DNA (gDNA) was co-incubated with the indicated purified protein in the presence (+) or absence (-) of $MgCl_2$ or EDTA for 5 min at 30°C. The results shown represent two independent experiments. **(B)** In vivo DNase activity. The integrity of gDNA was determined after its isolation from *E. coli* MG1655 cells in which the indicated proteins were expressed from arabinose-inducible expression plasmids; EV, empty plasmid. The results shown represent at least three independent experiments. **(C)** Quantification of *V. parahaemolyticus* RIMD 2210633 Δ*vpa1263-vti2* prey cells, constitutively expressing GFP, with no detectable DNA (green), DNA foci (orange), or DNA spread across the cell (cyan) after 3 h of competition against the indicated attacker strains. DNA was detected by Hoechst staining. The results represent the average ± SD of three independent experiments. In each experiment, at least 100 prey cells were randomly selected and manually evaluated per treatment. **(D)** Sample fluorescence microscope images of prey cells after 3 h competition against a Δ*hns* attacker strain, as described in **C**. Dashed yellow shapes in the DNA channel encircle prey cells detected in the GFP channel. Bar = 1 µm.

The MIX domain is necessary for T6SS-mediated secretion of VPA1263

After determining that its toxicity is mediated by DNase activity, we next sought to investigate the role of VPA1263's MIX domain. Since MIX domains are found at N-termini of diverse polymorphic toxins that are secreted by T6SS (Salomon *et al*, 2014a), we hypothesized that MIX plays a role in T6SS-mediated secretion. To test this, we monitored the T6SS1-mediated secretion of C-terminal Myc-His tagged VPA1263 variants expressed from a plasmid in a *V. parahaemolyticus* Δ*hns* strain with a constitutively active T6SS ($T6SS1^+$), or in a Δ*hns*/Δ*hcp1* mutant with an inactive T6SS1 ($T6SS1^-$). Notably, to avoid self-intoxication of strains over-expressing VPA1263 variants containing the HNH nuclease domain, we used the catalytically inactive mutant H837A (**Fig. 1E**). The full-length $VPA1263^{H837A}$ was secreted into the growth medium in a T6SS1-dependent manner, confirming previous comparative proteomics results (Salomon *et al*, 2014a) (**Fig. 3**). An N-terminal region, including the MIX and LysM domains ($VPA1263^{1-546}$), retained the ability to secrete via T6SS1, whereas the C-terminal region, containing the Pyocin_S and the HNH nuclease toxin domains ($VPA1263^{547-869/H837A}$), did not

(**Fig. 3**), indicating that the information required for T6SS1-mediated secretion is found at the N-terminal region. Remarkably, deletion of the region encoding amino acids 226-328 VPA1263$^{\Delta MIX/H837A}$), encompassing most of the MIX domain, resulted in loss of T6SS1-mediated secretion. This result suggests that MIX is required for T6SS1-mediated secretion of VPA1263. In support of this conclusion, replacing residues belonging to the invariant GxxY motif in the MIX domain (Salomon *et al*, 2014a) to alanine, i.e., glycine 246 and tyrosine 250 (VPA1263$^{G246A/H837A}$ and VPA1263$^{Y250A/H837A}$, respectively), also abolished VPA1263's secretion via T6SS1. Notably, we validated that T6SS1 was functional in the strains expressing the VPA1263 variants that were not secreted by detecting the T6SS1-mediated secretion of the hallmark T6SS protein, VgrG1 (**Fig. 3**). These results provide the first experimental indication that MIX is required for T6SS-mediated secretion of effectors. Attempts to determine whether MIX is sufficient to mediate secretion via T6SS were inconclusive, due to the low expression level of VPA1263 truncations containing only the MIX domain region.

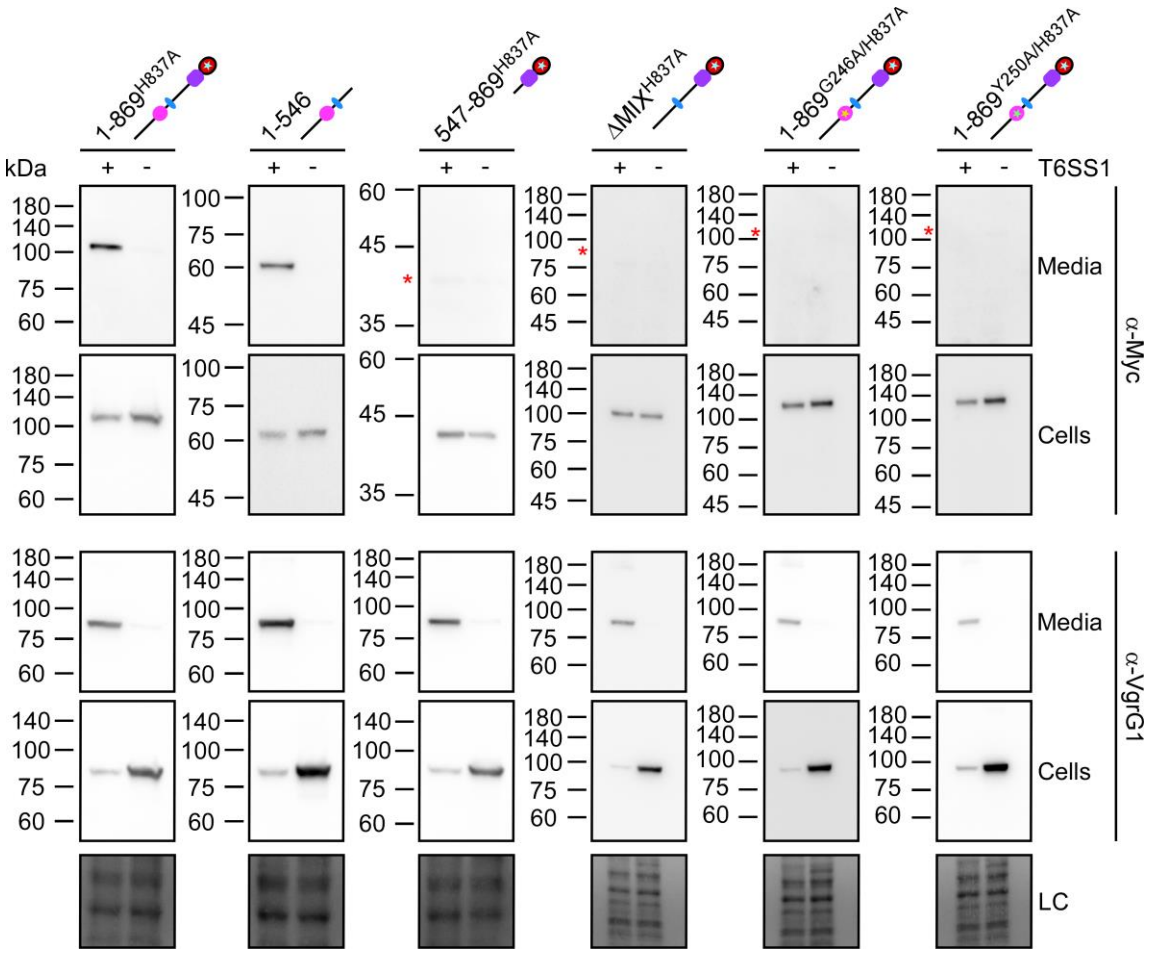

Figure 3. MIX is required for secretion of VPA1263 via T6SS1. Expression (cells) and secretion (media) of the indicated C-terminal Myc-His-tagged VPA1263 variants from *V. parahaemolyticus* RIMD 2210633 Δ*hns* (T6SS1^{+}) or Δ*hns*Δ*hcp1* (T6SS1^{-}). Proteins were expressed from an arabinose-inducible plasmid, and samples were resolved on SDS-PAGE. VPA1263 variants and the endogenous VgrG1 were visualized using specific antibodies against Myc and VgrG1, respectively. Schematic representations of the expressed VPA1263 variants are shown above; denoted domains and colors correspond to Figure 1B; stars denote point mutations in the expressed variant. Red asterisks denote the expected size of the indicated proteins in the media fractions. Loading control (LC) is shown for total protein lysates.

VPA1263 binds VgrG1 in a MIX-independent manner

T6SS effectors must be loaded onto the tail tube to be secreted. This can be achieved by interacting with either the Hcp, VgrG, or PAAR proteins (Jurėnas & Journet, 2021). To determine which tail tube component serves as the "loading platform" for VPA1263, we co-expressed FLAG-tagged VPA1263^{H837A} with Hcp1, VgrG1, or PAAR1 (VP1415$^{AHH/AAA}$; a mutant in which the toxin domain fused to the N-terminal PAAR domain is inactive (Jana *et al*, 2021)) in *E. coli*. A FLAG-tagged T6SS immunity protein, PoNi, from *V. parahaemolyticus* 12-297/B (Jana *et al*, 2019) was used as a negative control. Immunoprecipitation assays revealed that VPA1263 interacts specifically with VgrG1, but not with Hcp1 or PAAR1 (**Fig. 4A**). This result suggests that VPA1263 is loaded onto VgrG1 during T6SS1-mediated secretion.

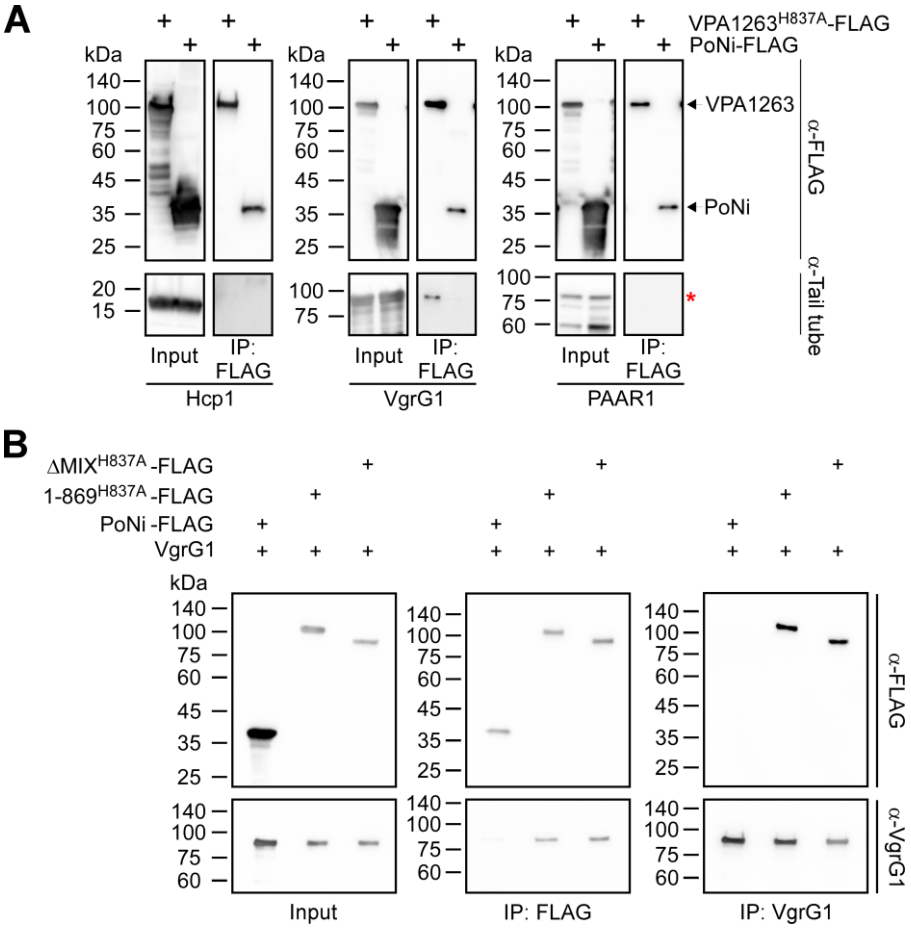

Figure 4. VPA1263 binds VgrG1 in a MIX-independent manner. (A) VPA1263 co-precipitates with VgrG1. Immunoprecipitation of FLAG-tagged VPA1263^{H837A} from *E. coli* co-expressing the tail tube components Hcp1, VgrG1, or PAAR1 (VP1415$^{AHH/AAA}$) using α-FLAG antibodies. Tail tube components were detected using custom-made specific antibodies, collectively referred to as α-Tail tube. An asterisk denotes the expected size of PAAR1. **(B)** MIX is not required for VPA1263's interaction with VgrG1. Immunoprecipitation of the indicated FLAG-tagged VPA1263 variants from *E. coli* co-expressing VgrG1 using either α-FLAG or α-VgrG1 antibodies. PoNi-FLAG was used as a negative control.

Since we showed that MIX is required for VPA1263 secretion, we next sought to determine whether MIX is also required for the interaction between VPA1263 and VgrG1. Surprisingly, a VPA1263 variant lacking the MIX domain (VPA1263$^{\Delta MIX/H837A}$) retained the ability to bind VgrG1 when both proteins were co-expressed in *E. coli* (**Fig. 4B**). This interaction was comparable to the one seen with the full-length VPA1263. Therefore, our

results suggest that VPA1263 binds to VgrG1 in a MIX-independent manner. Furthermore, since VPA1263$^{\Delta MIX/H837A}$ was not secreted in a T6SS1-dependent manner (**Fig. 3**), we also concluded that binding to a secreted T6SS tail tube component is insufficient to ensure T6SS-mediated secretion.

VpaI-6-like genomic islands carry diverse antibacterial and anti-phage weapons

VPA1263 is encoded on VPaI-6, a putative mobile element encompassing *vpa1254-vpa1270* (Hurley *et al*, 2006). When we analyzed the genetic composition of VpaI-6, we noted a Septu type I anti-phage defense system (Doron *et al*, 2018) encoded by *vpa1261* and *vpa1260* (**Fig. 1A** and **Fig. 5A**). In addition, we identified several genes that encoded putative DNA mobility elements, including *vpa1254* (transposase), *vpa1255* (helicase), *vpa1268* (GmtX), *vpa1269* (integrase), and *vpa1270* (GmtY) (Hurley *et al*, 2006) (**Fig. 1A**). To determine whether VpaI-6-like elements carry the same genetic cargo comprising a T6SS antibacterial effector and an anti-phage defense system, we aligned, using BLASTN, the nucleotide sequence of VpaI-6 against a database of 488 complete *Vibrio* RefSeq genomes (**Supplementary Dataset S1**). We found 126 *Vibrio* genomes that contained sequences homologous to VPaI-6 at various lengths (**Supplementary Dataset S2**). Analysis of the sequences revealed 22 genomes that contained VpaI-6-like genomic islands encompassing homologous sequences to the *vpa1268-vpa1270* genes located at the edge of VpaI-6 (**Supplementary Dataset S3**).

We identified nearly identical VpaI-6 genomic islands in a subset of *V. parahaemolyticus* genomes. Interestingly, VpaI-6-like genomic islands were found in various vibrios, including *V. alginolyticus*, *V. cholerae*, *V. vulnificus*, *V. natriegens*, *V. owensii*, *V. parahaemolyticus*, and others (**Fig. 5** and **Supplementary Dataset S4**). These genomic islands share close homology with the DNA mobility genes found at the edge of VpaI-6 (corresponding to *vpa1268-vpa1270*); however, the regions containing the cargo genes differ (**Fig. 5A**). Remarkably, of the nine VpaI-6-like variants that we identified (**Fig. 5A**; variants 2-10), four encoded one or two known anti-phage defense systems, and three encoded a known antibacterial T6SS effector and immunity pair in which the effector is fused to known T6SS-associated domains, such as MIX (Salomon *et al*, 2014a), FIX (Jana *et al*, 2019), or DUF4150 (PAAR) (Shneider *et al*, 2013) (**Fig. 5A**). Each genomic island variant seems to be restricted to one *Vibrio* strain and to be present only in a subset of this strain's genomes (**Fig. 5B**). Notably, several *V. alginolyticus* genomes contain two copies of the same genomic island variant: one on chromosome II and the other on a plasmid (**Fig. 5B** and **Supplementary Dataset S2**). Taken together, these results indicate that putative mobile genomic islands, which contain a backbone of mobility genes homologous to *vpa1268-vpa1270*, harbor a polymorphic cargo of antibacterial and anti-phage weapons.

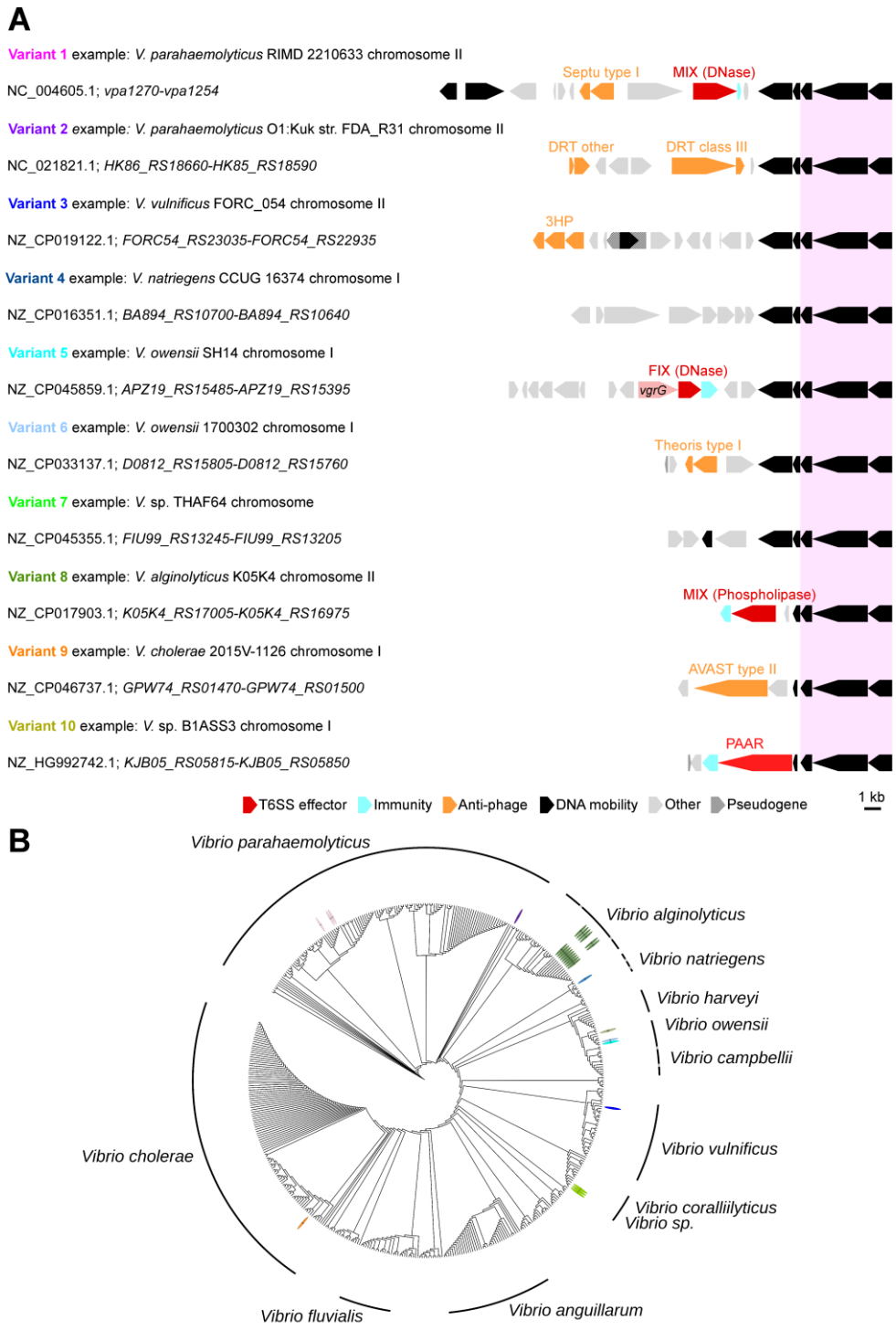

Figure 5. Antibacterial and anti-phage weapons in VpaI-6-like genomic islands. (A) Schematic representation of VpaI-6-like genomic islands identified in complete *Vibrio* genomes. Genes are denoted by arrows indicating the direction of transcription. Known anti-phage defense systems and T6SS effector and immunity pairs are denoted above according to their class and known activity (for T6SS effectors). Pink rectangles denote the region of homology between genes found in all VpaI-6 variants. The NCBI reference sequence number and the island border loci are denoted. **(B)** A phylogenetic tree of complete *Vibrio* genomes, based on the nucleotide sequence of *rpoB*. Genomes containing a VpaI-6 variant are denoted (ovals) according to the number of genomic islands that were identified; their colors correspond to variant colors shown in **A**.

229

DISCUSSION

In this work, we used the T6SS effector VPA1263 as a model to study different aspects of the class of polymorphic MIX-effectors. Our results revealed that the MIX domain is required for T6SS-mediated effector secretion, but that it is possibly dispensable for effector binding to the T6SS tail tube component, VgrG. Furthermore, we identified and demonstrated the activity of a DNase toxin domain belonging to the HNH nuclease superfamily, at the C-terminus of VPA1263.

The first report describing the MIX domain noted a genetic link between MIX-effectors and VgrG (Salomon *et al*, 2014a). Indeed, we show here that the MIX-effector, VPA1263, interacts with VgrG and not with the two other tail tube components, Hcp and PAAR. Nevertheless, although we expected to find that MIX plays a major role in mediating interaction with the tail tube, we did not observe a dramatic difference in the VgrG binding ability between the full-length effector and a variant lacking the MIX region. Notably, our results, which are based on the ectopic co-expression of the effector and VgrG1 in *E. coli*, cannot rule out the possibility that VPA1263 requires MIX for loading onto an assembled tail tube.

Importantly, we found that MIX is required for T6SS-mediated secretion; even single point mutations in the conserved central MIX motif, GxxY, were sufficient to abolish effector secretion, thus validating the importance of this motif. However, since MIX might not be required for effector loading onto the T6SS tail tube component, VgrG, the mechanism by which it contributes to secretion remains unknown. We speculate that MIX contributes toward a stable or desirable effector conformation that is required for correct loading or positioning on the tail tube. Alternatively, following recent observations by Liang *et al*, who suggested that effectors interact with T6SS components, such as TssK and TssF, to fulfill the requirement for the “stuffing model” (Liang *et al*, 2021), it is possible that MIX plays a role in mediating the interaction of a tail tube-loaded effector with the T6SS base plate. Inconclusive results obtained during repeated attempts to detect a MIX-mediated interaction between VPA1263 and TssK prevent us from currently confirming or ruling out this possibility.

Previous works suggested that the ability of proteins to bind tail tube components can be used as a method to identify T6SS effectors (Silverman *et al*, 2013; Howard *et al*, 2021; Lien & Lai, 2017). Although this can serve as a powerful method to reveal new effectors, our results, which show that proteins that are not secreted by T6SS can still bind tail tube components, underscore the need to validate such effector candidates by complementary methods (e.g., secretion assays or interbacterial competition assays). This is especially relevant when the interactions are identified upon protein over-expression in a surrogate bacterium or in the absence of an assembled tail tube.

In this work, we also investigated the antibacterial activity of VPA1263, and characterized a C-terminal DNase domain that mediates its toxicity during bacterial competition. The identified toxin belongs to the widespread and diverse HNH nuclease superfamily (Saravanan *et al*, 2004; Sano *et al*, 1993; Chak *et al*, 1991; Landthaler *et al*, 2004; Stoddard, 2005; Kala *et al*, 2014); it is found in various known and predicted bacterial toxins. Interestingly, in some instances this toxin domain is preceded by a Pyocin_S domain, as is the case in VPA1263. Pyocin_S was recently suggested to mediate the transport of DNase toxins across the inner-membrane, from the periplasm to cytoplasm (Atanaskovic *et al*, 2022). This activity was shown to be mediated by specific inner-membrane proteins that serve as receptors. It will be interesting to determine whether VPA1263 and other Pyocin_S-containing T6SS effectors require this domain for transport into the cytoplasm to mediate toxicity, since it remains unclear whether T6SS effectors are delivered directly into the recipient cell cytoplasm, periplasm, or randomly into either compartment (Vettiger & Basler, 2016; Quentin *et al*, 2018; Ho *et al*, 2017). Notably, we recently reported that VPA1263 selectively intoxicates bacterial strains when delivered via an engineered T6SS in *V. natriegens* (Jana *et al*, 2021). VPA1263-delivering attacker strains were toxic to *Vibrio* and *Aeromonas* strains, but had no effect on the viability of *E. coli* or *Salmonella* prey (Jana *et al*, 2021). It is therefore tempting

to speculate that differences in the potential inner-membrane receptors of the VPA1263 Pyocin_S domain are responsible for the observed selective toxicity. If true, it may represent a previously unappreciated mode of natural resistance against T6SS effectors.

Recent works showed that mobile genetic elements are hotspots for anti-phage defense systems (Rousset *et al*, 2022; Bernheim & Sorek, 2019; Johnson *et al*, 2022), and that T6SS effectors often reside in mobile elements (Salomon *et al*, 2015; Jana *et al*, 2019). A previous report also indicated that T6SS components, such as Hcp and VgrG, are encoded on excisable pathogenicity islands that also contain CRISPR-Cas systems (Carpenter *et al*, 2017). Here we found that VpaI-6 carries two weapon systems: an antibacterial T6SS effector (i.e., VPA1263) and an anti-phage defense system. We also showed that most VpaI-6-like genomic islands in vibrios harbor at least one of these weapons. Therefore, we concluded that VpaI-6-like genomic islands are hotspots for bacterial defensive weapons, either against attacking bacteriophages or against rival bacteria. It is possible that other genomic islands that were previously shown to be hotspots for anti-phage defense systems also harbor antibacterial weapons, such as T6SS effectors.

Our analysis to identify VpaI-6-like genomic islands was conservative, since it was performed only on complete RefSeq *Vibrio* genomes. Since the cassette corresponding to *vpa1268-vpa1270* is common to all VpaI-6-like genomic islands, we propose that it can be used to identify additional variants of this genomic island in other bacteria (e.g., in incomplete *Vibrio* genome and in non-*Vibrio* genomes) to reveal novel bacterial weapons. In that respect, VpaI-6-like variant 4, which is found in the T6SS-deficient *V. natriegens* and lacks any known defensive weapon, is of note since it may harbor a yet-to-be-identified anti-phage defense system.

MATERIALS AND METHODS

Strains and Media: For a complete list of strains used in this study, see **Supplementary Table S1**. *Escherichia coli* DH5α (λ pir) (a gift from Eric V. Stabb) was used for plasmid construction and maintenance. *E. coli* BL21 (DE3) was used for protein expression. *E. coli* MG1655 was used for effector toxicity assays and in vivo DNase assays. *E. coli* strains were grown in 2xYT broth (1.6% wt/vol tryptone, 1% wt/vol yeast extract, and 0.5% wt/vol NaCl) or on Lysogeny Broth (LB) agar plates containing 1% wt/vol NaCl at 37°C, or at 30°C when harboring effector expression plasmids. The media were supplemented with chloramphenicol (10 µg/mL) or kanamycin (30 µg/mL) to maintain plasmids, and with 0.4% wt/vol glucose to repress protein expression from the arabinose-inducible promoter, P*bad*. To induce expression from P*bad*, L-arabinose was added to media at 0.05-0.1% (wt/vol), as indicated.

Vibrio parahaemolyticus RIMD 2210633 (Makino *et al*, 2003) and its derivative strains, as well as *V. natriegens* ATCC 14048 were grown in MLB media (LB media containing 3% wt/vol NaCl) or on marine minimal media (MMM) agar plates (1.5% wt/vol agar, 2% wt/vol NaCl, 0.4% wt/vol galactose, 5 mM $MgSO_4$, 7 mM K_2SO_4, 77 mM K_2HPO_4, 35 mM KH_2PO_4, and 2 mM NH_4Cl) at 30°C. When vibrios contained a plasmid, the media were supplemented with kanamycin (250 µg/mL) or chloramphenicol (10 µg/mL) to maintain the plasmid. To induce expression from P*bad*, L-arabinose was added to media at 0.05% wt/vol.

Plasmid construction: For a complete list of plasmids used in this study, see **Supplementary Table S2**. For protein expression, the coding sequences (CDS) of *vpa1263* (BAC62606.1) and *vti2* (Chromosome 2, positions 1344453-1344737, GenBank number BA000032.2; encoding WP_005477334.1) were amplified from genomic DNA of *V. parahaemolyticus* RIMD 2210633. Amplification products were inserted into the multiple cloning site (MCS) of $pBAD^K$/Myc-His, or $pBAD33.1^F$ using the Gibson assembly method (Gibson *et al*, 2009). Plasmids were introduced into *E. coli* using electroporation. Transformants were grown on agar plates supplemented with 0.4% wt/vol glucose to repress unwanted expression from the P*bad* promotor during the subcloning steps. Plasmids were

introduced into *V. parahaemolyticus* via conjugation. Transconjugants were grown on MMM agar plates supplemented with appropriate antibiotics to maintain the plasmids.

Construction of deletion strains: The construction of pDM4-based (O'Toole *et al*, 1996) plasmids for deletion of *vpa1263*, *vpa1263-vti2*, and *hns* (*vp1133*) was reported previously (Salomon *et al*, 2014b, 2014a). In-frame deletions of *vpa1263*, *vpa1263-vti2*, and *hns* in *V. parahaemolyticus* RIMD 2210633 were performed as previously described (Salomon *et al*, 2013).

Toxicity in *E. coli*: Bacterial toxicity assays were performed as previously described (Dar *et al*, 2021), with minor changes. Briefly, to assess the toxicity mediated by VPA1263 or its truncated versions, pBAD^{K}/Myc-His plasmids encoding the indicated proteins were transformed into *E. coli* MG1655. *E. coli* transformants were streaked onto either repressing (containing 0.4% wt/vol glucose) or inducing (containing 0.05% wt/vol L-arabinose) LB agar plates supplemented with kanamycin. Chloramphenicol was also included in the media when a pBAD33.1^{F}-based plasmid was used. Plates were incubated at 30°C for 16 hours, and then imaged using a Fusion FX6 imaging system (Vilber Lourmat). The experiments were performed at least three times with similar results. Results from a representative experiment are shown.

Protein expression in *E. coli*: Protein expression in *E. coli* was performed as previously described (Dar *et al*, 2021), with minor changes. Briefly, to assess the expression of C-terminal Myc-tagged proteins encoded on arabinose-inducible plasmids, overnight cultures of *E. coli* MG1655 strains containing the indicated plasmids were washed twice with fresh 2xYT broth to remove residual glucose. Following normalization to OD_{600} = 0.5 in 3 mL of 2xYT broth supplemented with appropriate antibiotics, cultures were grown for 2 hours at 37°C. To induce protein expression, 0.05% (wt/vol) L-arabinose was added to the media. After having grown for 2 additional hours at 37°C, 0.5 OD_{600} units of cells were pelleted and resuspended in (2X) Tris-Glycine SDS sample buffer (Novex, Life Sciences). Samples were boiled for 5 min, and cell lysates were resolved on Mini-PROTEAN or criterion TGX Stain-Free™ precast gels (Bio-Rad). For immunoblotting, α-Myc antibodies (Santa Cruz Biotechnology, 9E10, mouse mAb; sc-40) were used at 1:1,000 dilution. Protein signals were visualized in a Fusion FX6 imaging system (Vilber Lourmat) using enhanced chemiluminescence (ECL) reagents.

Protein purification: To purify truncated VPA1263 proteins for the in vitro DNase assays, *E. coli* BL21 (DE3) cells harboring plasmids for the arabinose-inducible expression of the indicated Myc-His-tagged VPA1263 variants and the FLAG-tagged Vti2 (the immunity protein required to antagonize the toxicity of VPA1263 variants inside bacteria) were grown for 16 hours in 2xYT media supplemented with kanamycin and chloramphenicol at 37°C. Bacterial cultures were then diluted 100-fold into fresh media and incubated at 37°C with agitation (180 rpm). When bacterial cultures reached an OD_{600} of ~ 1.0, L-arabinose was added to the media (to a final concentration of 0.1% (wt/vol)) to induce protein expression, and cultures were grown for 4 additional hours at 30°C. Cells were harvested by centrifugation at 4°C (20 min at 13,300 x *g*), followed by washing with a 0.9% (wt/vol) NaCl solution to remove residual media. Then, cells were resuspended in 3 mL lysis buffer A (20 mM Tris-Cl pH 7.5, 500 mM NaCl, 5% vol/vol glycerol, 10 mM imidazole, 0.1 mM PMSF, and 8 M urea). Urea was included in the buffer to denature the proteins and thus release Vti2 from the VPA1263 variants. Cells were disrupted using a high-pressure cell disruptor (Constant system One Shot cell disruptor, model code: MC/AA). To remove cell debris, lysates were centrifuged for 20 min at 13,300 x *g* at 4°C. Next, 250 µL of Ni-Sepharose resin (50% slurry; GE healthcare) were pre-washed with lysis buffer A and then mixed with the supernatant fractions of lysed cells containing the denatured proteins. The suspensions were incubated for one hour at 4°C with constant rotation, and then loaded onto a column. Immobilized resin was washed with 10 mL wash buffer A (20 mM Tris-Cl pH 7.5, 500 mM NaCl, 5% vol/vol glycerol, 40 mM imidazole, and 8 M urea). Bound proteins were eluted from the column using 1 mL elution buffer A (20 mM Tris-Cl pH 7.5, 500 mM NaCl, 5% vol/vol glycerol, 500 mM imidazole, and 8 M urea).

The presence and purity of the eluted Myc-His-tagged VPA1263 variants were confirmed by SDS-PAGE, using stain-free gels (Bio-rad).

To refold the denatured, purified proteins before in vitro DNase activity assays, a refolding procedure was applied. The eluted proteins were dialyzed against DNase assay buffer (20 mM Tris-Cl pH 7.5, 200 mM NaCl, 5% vol/vol glycerol) and incubated for an hour at 4°C. The buffer was replaced twice to remove unwanted imidazole and urea. Then, the 1 mL suspension was concentrated to ~ 300 µL using a Spin-X UF concentrator column (Corning, 30 kDa). The purified proteins were quantified by the Bradford method using 5X Bradford reagent (Bio-rad). The all procedure was carried out at 4°C.

In vitro DNase assays: For determining in vitro DNase activity, genomic DNA isolated from *E. coli* BL21(DE3) (200 ng) was incubated with 0.5 µg of purified VPA1263 variants for 5 min at 30°C in DNase assay buffer (20 mM Tris-Cl pH 7.5, 200 mM NaCl, 5% vol/vol glycerol) supplemented with either 2 mM EDTA (a metal chelator) or $MgCl_2$. The total volume of the reactions was 20 µL. The reactions were stopped by adding 6.65 µg of Proteinase K and the samples were incubated for 5 min at 55°C. Samples were analyzed by 1.0% agarose-gel electrophoresis. For positive and negative controls, 1 U DNase I (Thermo Fisher Scientific) and 0.5 µg BSA (Sigma) were used, respectively. The experiments were performed twice with similar results. Results from a representative experiment are shown.

In vivo DNase assays: *E. coli* MG1655 strains containing the indicated $pBAD^{K}$/Myc-His plasmid, either empty or encoding $VPA1263^{547\text{-}869}$, $VPA1263^{547\text{-}869/H837A}$, or $PoNe^{Bc}$ (BC3021), were grown overnight in 2xYT media supplemented with kanamycin and 0.4% (wt/vol) glucose. Overnight cultures were washed with 2xYT media and normalized to an OD_{600} of 1.0 in 3 mL of fresh 2xYT supplemented with kanamycin and 0.1% (wt/vol) L-arabinose (to induce protein expression). Cultures were grown for 90 min with agitation (220 rpm) at 37°C before 1.0 OD_{600} units were pelleted. Genomic DNA was isolated from each sample using the EZ spin column genomic DNA kit (Bio Basic) and eluted with 30 µL of sterile distilled water (Milli-Q). Equal genomic DNA elution volumes were analyzed by 1.0% (wt/vol) agarose gel electrophoresis. The experiments were performed at least three times with similar results. Results from a representative experiment are shown.

***Vibrio* growth assays:** *Vibrio* growth assays were performed as previously described (Dar *et al*, 2021). Briefly, overnight cultures of *V. parahaemolyticus* strains were normalized to $OD_{600} = 0.01$ in MLB and transferred to 96-well plates (200 µL per well; $n = 3$ technical replicates). The 96-well plates were incubated in a microplate reader (BioTek SYNERGY H1) at 30°C with constant shaking at 205 cpm. OD_{600} reads were acquired every 10 min. The experiments were performed at least three times with similar results. Results from a representative experiment are shown.

Bacterial competition assays: Bacterial competition assays were performed as previously described (Dar *et al*, 2021). Briefly, attacker and prey strains were grown overnight in MLB with the addition of antibiotics when maintenance of plasmids was required. Bacterial cultures were normalized to $OD_{600} = 0.5$, and mixed at a 4:1 (attacker:prey) ratio. The mixtures were spotted on MLB agar plates and incubated for 4 hours at 30°C. Colony forming units (CFU) of the prey strain were determined by growing the mixtures on selective plates at the 0 and 4-hour timepoints. The experiments were performed at least three times with similar results. Results from a representative experiment are shown.

Fluorescence microscopy: Assessment of prey DNA morphology during bacterial competition was performed as previously described (Jana *et al*, 2019). Briefly, the indicated *V. parahaemolyticus* RIMD 2210633 strains were grown overnight and mixed as described above for the bacterial competition assays. The Δ*vpa1263-vti2* prey strain constitutively expressed GFP (from a stable, high copy number plasmid (Ritchie *et al*, 2012)) to distinguish them from attacker cells. Attacker:prey mixtures were spotted on MLB agar plates and incubated at 30°C for 3 hours. Bacteria were then scraped from the plates, washed with M9 media, and incubated at room temperature for 10 min in M9 media containing the Hoechst

33342 (Invitrogen) DNA dye at a final concentration of 1 µg/µL. The cells were then washed and resuspended in 30 µL M9 media. One microliter of bacterial suspensions was spotted onto M9 agar (1.5% wt/vol) pads and allowed to dry for 2 min before the pads were placed face-down in 35 mm glass bottom Cellview cell culture dishes. Bacteria were imaged in a Nikon Eclipse Ti2-E inverted motorized microscope equipped with a CFI PLAN apochromat DM 100X oil lambda PH-3 (NA, 1.45) objective lens, a Lumencor SOLA SE II 395 light source, and ET-DAPI (#49028, used to visualize Hoechst signal) and ET-EGFP (#49002, used to visualize GFP signal) filter sets. Images were acquired using a DS-QI2 Mono cooled digital microscope camera (16 MP), and were post-processed using Fiji ImageJ suite. Cells exhibiting the indicated DNA morphologies were manually counted (> 100 GFP-expressing prey cells per treatment in each experiment). The experiment was repeated three times.

Protein secretion assays: *Vibrio parahaemolyticus* RIMD 2210633 strains were grown overnight at 30°C in MLB supplemented with kanamycin to maintain plasmids. Bacterial cultures were normalized to OD_{600} = 0.18 in 5 mL MLB supplemented with kanamycin and L-arabinose (0.05% wt/vol) to induce expression from P*bad* promoters. After 4 hours of incubation at 30°C with agitation (220 rpm), 1.0 OD_{600} units of cells were collected for expression fractions (cells). The cell pellets were resuspended in (2X) Tris-Glycine SDS sample buffer (Novex, Life Sciences). For secretion fractions (media), suspension volumes equivalent to 10 OD_{600} units of cells were filtered (0.22 µm), and proteins were precipitated from the media using deoxycholate and trichloroacetic acid (Bensadoun & Weinstein, 1976). Cold acetone was used to wash the protein precipitates twice. Then, protein precipitates were resuspended in 20 µL of 10 mM Tris-HCl pH = 8, followed by the addition of 20 µL of (2X) Tris-Glycine SDS Sample Buffer supplemented with 5% β-mercaptoethanol and 0.5 µL 1 N NaOH to maintain a basic pH. Expression and secretion samples were boiled for 5 min and then resolved on Mini-PROTEAN or Criterion™ TGX Stain-Free™ precast gels (Bio-Rad). For immunoblotting, primary antibodies were used at a 1:1000 concentration. The following antibodies were used: α-Myc antibodies (Santa Cruz Biotechnology, 9E10, mouse mAb; sc-40), and custom-made α-VgrG1 (Li *et al*, 2017). Protein signals were visualized in a Fusion FX6 imaging system (Vilber Lourmat) using enhanced chemiluminescence (ECL) reagents.

Co-immunoprecipitation assays: To determine whether VPA1263 variants directly interact with the tail tube components Hcp1 (VP1393), VgrG1 (VP1394), or PAAR (VP1415 containing mutations in its predicted toxin active site (Jana *et al*, 2021); $VP1415^{AHH/AAA}$), *E. coli* BL21 (DE3) cells harboring $pBAD33.1^{F}$-based plasmids encoding C-terminal FLAG-tagged $PoNi^{VP}$ (B5C30_RS14460) or the indicated VPA1263 variants, together with $pBAD^{K}$/Myc-His-based plasmids encoding untagged Hcp1, VgrG1, or $VP1415^{AHH/AAA}$ were grown overnight in 2xYT media supplemented with kanamycin and chloramphenicol at 37°C. Overnight cultures were diluted 1:100 in fresh 2xYT media supplemented with the appropriate antibiotics, and grown at 37°C for 2 hours. Then, 0.1% (wt/vol) L-arabinose was added to the media to induce protein expression, and cultures were grown at 30°C for 4 more hours. Next, 100 OD_{600} units of cells were pelleted by centrifugation at 3,500 x *g* for 10 min at 4°C. Cell pellets were resuspended in 3 mL of Lysis buffer B (150 mM NaCl, 20 mM Tris-HCl pH = 7.5, 1 mM EDTA, and 0.5% [vol/vol] NP-40) supplemented with 0.1 mM PMSF, and lysed using a high-pressure cell disruptor (Constant system One Shot cell disruptor, model code: MC/AA). Cell debris was removed by centrifugation at 15,000 x *g* for 20 min at 4°C. Next, 500 µL of the cleared supernatants were mixed with 10 µL of DYKDDDDK Tag antibody (D6W5B rabbit mAb #14793; Cell Signaling Technology; the antibody binds to the same epitope as Sigma's α-FLAG M2 Antibody, and is therefore referred to here as α-FLAG) or α-VgrG1 and incubated for one hour at 4°C with constant rotation. A 1:1 mixture of protein A and protein G magnetic beads (New England BioLabs), prewashed with Lysis buffer B, was then added to the supernatant samples, followed by a one-hour incubation at 4°C with constant rotation. The beads were then washed eight times with 200 µL Lysis buffer B. Finally, the beads were collected, and bound proteins were eluted by adding 100 µL of (2X) Tris-Glycine SDS Sample Buffer, supplemented with 10% β-mercaptoethanol, followed by heating at 70°C for 5 min. Samples were analyzed by immunoblotting as mentioned above. The following antibodies

were used: DYKDDDDK Tag Antibody (α-FLAG), custom-made α-VgrG1 (Li *et al*, 2017), and custom-made α-VP1415 and α-Hcp1 (polyclonal antibodies were raised in rabbit against the peptides CSKSTGDAGGDKKGV and CGTAGNDDWRAPREA, respectively; the cysteines at the end of the peptides were added during the synthesis process and are not found in the endogenous protein; GenScript). HRP-conjugated α-Light Chain-specific secondary antibodies (Jackson ImmunoResearch) were used to avoid detecting the primary antibodies' heavy chains.

VPA1263 domain and homologs analysis: Domains in VPA1263 (BAC62606.1) were identified using the NCBI conserved domain database (Marchler-Bauer *et al*, 2007) or by homology detection and structure prediction using a hidden Markov model (HMM)-HMM comparison, i.e., the HHpred tool (Zimmermann *et al*, 2018). Proteins containing a specialized secretion system delivery domain or known secreted toxins bearing homology to the C-terminal HNH nuclease toxin domain of VPA1263 were identified through an iterative search against the UniProt protein sequence database using Jackhmmer (Potter *et al*, 2018). Homologs containing diverse secretion-associated domains (e.g., domains found in T6SS or T7SS polymorphic toxins) were selected, and their C-terminal ends were aligned in MEGA X (Kumar *et al*, 2018) using MUSCLE (Edgar, 2004); alignment columns not represented in VPA1263 were removed. Conserved residues were illustrated using the WebLogo 3 server (Crooks *et al*, 2004). Amino acid numbering was based on the sequence of VPA1263.

Identifying VpaI-6-like genomic islands and analysis of cargo genes: Bacterial RefSeq genomes were downloaded from NCBI on January 21, 2022, and a database of *Vibrio* complete genomes (assembly level "chromosome" or higher) was constructed (**Supplementary Database S1**). The nucleotide sequence of VpaI-6 was aligned against the database was performed using BLASTN (an expect value threshold of 10^{-12} was used) (**Supplementary Database S2**). The BLASTN hits were visualized by plotting the genomic accessions against VpaI-6 (**Supplementary Database S3**). Briefly, hits of the same genomic accession were merged if the hits were found on the same strand and the distance between hits was less than 30,000 bp. For each position of the genomic accession, the percent identity to VpaI-6 was denoted. The borders of VpaI-6-like genomic islands were determined by aligning flanking sequences against closely related bacterial genomes lacking a VpaI-6-like genomic island (**Supplementary Database S4**). Anti-phage defense systems within VpaI-6-like variants were identified using the Prokaryotic Antiviral Defense LOCator (PADLOC) webserver (https://padloc.otago.ac.nz/padloc/) (Payne *et al*, 2021).

Constructing a phylogenetic tree of complete *Vibrio* genomes: Nucleotide sequences of the *rpoB* gene were aligned using the MAFFT v7 FFT-NS-i program (Katoh *et al*, 2018, 2002). The evolutionary history was inferred using the neighbor-joining method (Saitou & Nei, 1987) with the Jukes-Cantor substitution model (JC69). The analysis included 486 complete or nearly complete nucleotide sequences and 3,971 conserved sites. The phylogenetic analysis was conducted using the MAFFT server (mafft.cbrc.jp/alignment/server/) and the resulting tree was visualized using iTOL (Letunic & Bork, 2021).

ACKNOWLEDGMENTS

This project received funding from the European Research Council under the European Union's Horizon 2020 research and innovation program (grant agreement no. 714224), and from the Israel Science Foundation (grant no. 920/17) to D Salomon. CM Fridman was supported by scholarships from the Clore Israel Foundation and from the Manna Center Program in Food Safety and Security at Tel Aviv University. We thank members of the Salomon lab for helpful discussions and suggestions, and Dan Goldenberg for technical assistance. This work was performed in partial fulfillment of the requirements for a PhD degree for CM Fridman at the Sackler Faculty of Medicine, Tel Aviv University.

AUTHOR CONTRIBUTIONS

CM Fridman: conceptualization, investigation, methodology, and writing—original draft.

B Jana: conceptualization, investigation, methodology, and writing—review and editing.

R Ben-Yaakov: investigation and methodology.

E Bosis: conceptualization, investigation, methodology, and writing—review and editing.

D Salomon: conceptualization, supervision, funding acquisition, investigation, methodology, and writing—original draft.

CONFLICT OF INTEREST

The authors declare that they have no conflict of interest.

REFERENCES

Alcoforado Diniz J & Coulthurst SJ (2015) Intraspecies Competition in Serratia marcescens Is Mediated by Type VI-Secreted Rhs Effectors and a Conserved Effector-Associated Accessory Protein. *J Bacteriol* 197: 2350–60

Aoki SK, Diner EJ, de Roodenbeke C t'Kint, Burgess BR, Poole SJ, Braaten BA, Jones AM, Webb JS, Hayes CS, Cotter PA, *et al* (2010) A widespread family of polymorphic contact-dependent toxin delivery systems in bacteria. *Nature* 468: 439–442

Atanaskovic I, Sharp C, Press C, Kaminska R & Kleanthous C (2022) Bacterial Competition Systems Share a Domain Required for Inner Membrane Transport of the Bacteriocin Pyocin G from Pseudomonas aeruginosa. *MBio* 13: e0339621

Basler M, Pilhofer M, Henderson GP, Jensen GJ & Mekalanos JJ (2012) Type VI secretion requires a dynamic contractile phage tail-like structure. *Nature* 483: 182–6

Bensadoun A & Weinstein D (1976) Assay of proteins in the presence of interfering materials. *Anal Biochem* 70: 241–250

Bernheim A & Sorek R (2019) The pan-immune system of bacteria: antiviral defence as a community resource. *Nat Rev Microbiol*: 1–7

Bondage DD, Lin J-S, Ma L-S, Kuo C-H & Lai E-M (2016) VgrG C terminus confers the type VI effector transport specificity and is required for binding with PAAR and adaptor–effector complex. *Proc Natl Acad Sci* 113: E3931–E3940

Boyer F, Fichant G, Berthod J, Vandenbrouck Y & Attree I (2009) Dissecting the bacterial type VI secretion system by a genome wide in silico analysis: What can be learned from available microbial genomic resources? *BMC Genomics* 10: 104

Buist G, Steen A, Kok J & Kuipers OP (2008) LysM, a widely distributed protein motif for binding to (peptido)glycans. *Mol Microbiol* 68: 838–847

Burkinshaw BJ, Liang X, Wong M, Le ANH, Lam L & Dong TG (2018) A type VI secretion system effector delivery mechanism dependent on PAAR and a chaperone-co-chaperone complex. *Nat Microbiol* 3: 632–640

Carpenter MR, Kalburge SS, Borowski JD, Peters MC, Colwell RR & Boyd EF (2017) CRISPR-Cas and contact-dependent secretion systems present on excisable pathogenicity islands with conserved recombination modules. *J Bacteriol* 199: e00842-16

Chak KF, Kuo WS, Lu FM & James R (1991) Cloning and characterization of the ColE7 plasmid. *J Gen Microbiol* 137: 91–100

Cianfanelli FR, Alcoforado Diniz J, Guo M, De Cesare V, Trost M & Coulthurst SJ (2016) VgrG and PAAR proteins define distinct versions of a functional type VI secretion system. *PLoS Pathog* 12: 1–27

Crooks GE, Hon G, Chandonia J-M & Brenner SE (2004) WebLogo: a sequence logo generator. *Genome Res* 14: 1188–90

Dar Y, Jana B, Bosis E & Salomon D (2021) A binary effector module secreted by a type VI secretion system. *EMBO Rep*: e53981

Dar Y, Salomon D & Bosis E (2018) The antibacterial and anti-eukaryotic Type VI secretion system MIX-effector repertoire in Vibrionaceae. *Mar Drugs* 16: 433

Doron S, Melamed S, Ofir G, Leavitt A, Lopatina A, Keren M, Amitai G & Sorek R (2018) Systematic discovery of antiphage defense systems in the microbial pangenome. *Science* 359: eaar4120

Edgar RC (2004) MUSCLE: multiple sequence alignment with high accuracy and high throughput. *Nucleic Acids Res* 32: 1792–1797

Gibson DG, Young L, Chuang RY, Venter JC, Hutchison CA & Smith HO (2009) Enzymatic assembly of DNA molecules up to several hundred kilobases. *Nat Methods* 6: 343–345

Hachani A, Allsopp LP, Oduko Y & Filloux A (2014) The VgrG proteins are 'à la carte' delivery systems for bacterial type VI effectors. *J Biol Chem* 289: 17872–84

Ho BT, Fu Y, Dong TG & Mekalanos JJ (2017) *Vibrio cholerae* type 6 secretion system effector trafficking in target bacterial cells. *Proc Natl Acad Sci*: 201711219

Hood RD, Singh P, Hsu FS, Güvener T, Carl MA, Trinidad RRS, Silverman JM, Ohlson BB, Hicks KG, Plemel RL, *et al* (2010) A type VI secretion system of Pseudomonas aeruginosa targets a toxin to bacteria. *Cell Host Microbe* 7: 25–37

Howard SA, Furniss RCD, Bonini D, Amin H, Paracuellos P, Zlotkin D, Costa TRD, Levy A, Mavridou DAI & Filloux A (2021) The breadth and molecular basis of hcp-driven type vi secretion system effector delivery. *MBio* 12: e0026221

Hurley CC, Quirke AM, Reen FJ & Boyd EF (2006) Four genomic islands that mark post-1995 pandemic Vibrio parahaemolyticus isolates. *BMC Genomics* 7: 104

Jamet A & Nassif X (2015) New players in the toxin field: polymorphic toxin systems in bacteria. *MBio* 6: e00285-15

Jana B, Fridman CM, Bosis E & Salomon D (2019) A modular effector with a DNase domain and a marker for T6SS substrates. *Nat Commun* 10: 3595

Jana B, Keppel K & Salomon D (2021) Engineering a customizable antibacterial T6SS-based platform in Vibrio natriegens. *EMBO Rep* 22: e53681

Jana B & Salomon D (2019) Type VI secretion system: a modular toolkit for bacterial dominance. *Future Microbiol* 14: fmb-2019-0194

Johnson CM, Harden MM & Grossman AD (2022) Interactions between mobile genetic elements: An anti-phage gene in an integrative and conjugative element protects host cells from predation by a temperate bacteriophage. *PLOS Genet* 18: e1010065

Jurėnas D & Journet L (2021) Activity, delivery, and diversity of Type VI secretion effectors. *Mol Microbiol* 115: 383–394

Kala S, Cumby N, Sadowski PD, Hyder BZ, Kanelis V, Davidson AR & Maxwell KL (2014) HNH proteins are a widespread component of phage DNA packaging machines. *Proc Natl Acad Sci U S A* 111: 6022–7

Katoh K, Misawa K, Kuma K & Miyata T (2002) MAFFT: a novel method for rapid multiple sequence alignment based on fast Fourier transform. *Nucleic Acids Res* 30: 3059–66

Katoh K, Rozewicki J & Yamada KD (2018) MAFFT online service: Multiple sequence alignment, interactive sequence choice and visualization. *Brief Bioinform* 20: 1160–1166

Klein A, Wojdyla JA, Joshi A, Josts I, McCaughey LC, Housden NG, Kaminska R, Byron O, Walker D & Kleanthous C (2016) Structural and biophysical analysis of nuclease protein antibiotics. *Biochem J* 473: 2799–812

Koskiniemi S, Lamoureux JG, Nikolakakis KC, t'Kint de Roodenbeke C, Kaplan MD, Low DA & Hayes CS (2013) Rhs proteins from diverse bacteria mediate intercellular competition. *Proc Natl Acad Sci U S A* 110: 7032–7

Kumar S, Stecher G, Li M, Knyaz C & Tamura K (2018) MEGA X: Molecular evolutionary genetics analysis across computing platforms. *Mol Biol Evol* 35: 1547–1549

Landthaler M, Lau NC & Shub DA (2004) Group I intron homing in Bacillus phages SPO1 and SP82: A gene conversion event initiated by a nicking homing endonuclease. *J Bacteriol* 186

Letunic I & Bork P (2021) Interactive tree of life (iTOL) v5: An online tool for phylogenetic tree display and annotation. *Nucleic Acids Res* 49: W293–W296

Li P, Kinch LN, Ray A, Dalia AB, Cong Q, Nunan LM, Camilli A, Grishin N V, Salomon D & Orth K (2017) Acute hepatopancreatic necrosis disease-causing Vibrio parahaemolyticus strains maintain an antibacterial type VI secretion system with versatile effector repertoires. *Appl Environ Microbiol* 83: e00737-17

Liang X, Moore R, Wilton M, Wong MJQ, Lam L & Dong TG (2015) Identification of divergent type VI secretion effectors using a conserved chaperone domain. *Proc Natl Acad Sci* 112: 9106–9111

Liang X, Pei TT, Li H, Zheng HY, Luo H, Cui Y, Tang MX, Zhao YJ, Xu P & Dong T (2021) VgrG-dependent effectors and chaperones modulate the assembly of the type VI secretion system. *PLoS Pathog* 17: e1010116

Lien YW & Lai EM (2017) Type VI secretion effectors: Methodologies and biology. *Front Cell Infect Microbiol* 7: 254

Makino K, Oshima K, Kurokawa K, Yokoyama K, Uda T, Tagomori K, Iijima Y, Najima M, Nakano M, Yamashita A, *et al* (2003) Genome sequence of Vibrio parahaemolyticus: a pathogenic mechanism distinct from that of V cholerae. *Lancet* 361: 743–749

Marchler-Bauer A, Anderson JB, Derbyshire MK, DeWeese-Scott C, Gonzales NR, Gwadz M, Hao L, He S, Hurwitz DI, Jackson JD, *et al* (2007) CDD: a conserved domain database for interactive domain family analysis. *Nucleic Acids Res* 35: D237-40

Michel-Briand Y & Baysse C (2002) The pyocins of Pseudomonas aeruginosa. *Biochimie* 84: 499–510

Miyata ST, Kitaoka M, Brooks TM, McAuley SB & Pukatzki S (2011) Vibrio cholerae requires the type VI secretion system virulence factor vasx to kill dictyostelium discoideum. *Infect Immun* 79: 2941–2949

O'Toole R, Milton DL & Wolf-Watz H (1996) Chemotactic motility is required for invasion of the host by the fish pathogen Vibrio anguillarum. *Mol Microbiol* 19: 625–637

Payne LJ, Todeschini TC, Wu Y, Perry BJ, Ronson CW, Fineran PC, Nobrega FL & Jackson SA (2021) Identification and classification of antiviral defence systems in bacteria and archaea with PADLOC reveals new system types. *Nucleic Acids Res* 49: 10868–10878

Potter SC, Luciani A, Eddy SR, Park Y, Lopez R & Finn RD (2018) HMMER web server: 2018 update. *Nucleic Acids Res* 46: W200–W204

Poulsen C, Panjikar S, Holton SJ, Wilmanns M & Song Y-H (2014) WXG100 Protein

Superfamily Consists of Three Subfamilies and Exhibits an α-Helical C-Terminal Conserved Residue Pattern. *PLoS One* 9: e89313

Pukatzki S, Ma AT, Sturtevant D, Krastins B, Sarracino D, Nelson WC, Heidelberg JF & Mekalanos JJ (2006) Identification of a conserved bacterial protein secretion system in Vibrio cholerae using the Dictyostelium host model system. *Proc Natl Acad Sci* 103: 1528–1533

Quentin D, Ahmad S, Shanthamoorthy P, Mougous JD, Whitney JC & Raunser S (2018) Mechanism of loading and translocation of type VI secretion system effector Tse6. *Nat Microbiol* 3: 1142–1152

Ray A, Schwartz N, Souza Santos M, Zhang J, Orth K, Salomon D, de Souza Santos M, Zhang J, Orth K & Salomon D (2017) Type VI secretion system MIX-effectors carry both antibacterial and anti-eukaryotic activities. *EMBO Rep* 18: e201744226

Ritchie JM, Rui H, Zhou X, Iida T, Kodoma T, Ito S, Davis BM, Bronson RT & Waldor MK (2012) Inflammation and Disintegration of Intestinal Villi in an Experimental Model for Vibrio parahaemolyticus-Induced Diarrhea. *PLoS Pathog* 8: e1002593

Rousset F, Depardieu F, Miele S, Dowding J, Laval A-L, Lieberman E, Garry D, Rocha EPC, Bernheim A & Bikard D (2022) Phages and their satellites encode hotspots of antiviral systems. *Cell Host Microbe*

Ruhe ZC, Low DA & Hayes CS (2020) Polymorphic Toxins and Their Immunity Proteins: Diversity, Evolution, and Mechanisms of Delivery. *Annu Rev Microbiol* 74: 497–520

Russell AB, Singh P, Brittnacher M, Bui NK, Hood RD, Carl MA, Agnello DM, Schwarz S, Goodlett DR, Vollmer W, *et al* (2012) A widespread bacterial type VI secretion effector superfamily identified using a heuristic approach. *Cell Host Microbe* 11: 538–549

Saitou N & Nei M (1987) The neighbor-joining method: a new method for reconstructing phylogenetic trees. *Mol Biol Evol* 4: 406–425

Salomon D, Gonzalez H, Updegraff BL & Orth K (2013) Vibrio parahaemolyticus Type VI secretion system 1 Is activated in marine conditions to target bacteria, and is differentially regulated from system 2. *PLoS One* 8: e61086

Salomon D, Kinch LN, Trudgian DC, Guo X, Klimko JA, Grishin N V., Mirzaei H & Orth K (2014a) Marker for type VI secretion system effectors. *Proc Natl Acad Sci* 111: 9271–9276

Salomon D, Klimko JA & Orth K (2014b) H-NS regulates the Vibrio parahaemolyticus type VI secretion system 1. *Microbiol (United Kingdom)* 160: 1867–1873

Salomon D, Klimko JA, Trudgian DC, Kinch LN, Grishin N V., Mirzaei H & Orth K (2015) Type VI secretion system toxins horizontally shared between marine bacteria. *PLoS Pathog* 11: 1–20

Sano Y, Matsui H, Kobayashi M & Kageyama M (1993) Molecular structures and functions of pyocins S1 and S2 in Pseudomonas aeruginosa. *J Bacteriol* 175: 2907–2916

Saravanan M, Bujnicki JM, Cymerman IA, Rao DN & Nagaraja V (2004) Type II restriction endonuclease R.Kpnl is a member of the HNH nuclease superfamily. *Nucleic Acids Res* 32: 6129–6135

Shneider MM, Buth SA, Ho BT, Basler M, Mekalanos JJ & Leiman PG (2013) PAAR-repeat proteins sharpen and diversify the type VI secretion system spike. *Nature* 500: 350–353

Silverman JM, Agnello DM, Zheng H, Andrews BT, Li M, Catalano CE, Gonen T & Mougous JD (2013) Haemolysin coregulated protein is an exported receptor and chaperone of type VI secretion substrates. *Mol Cell* 51: 584–593

Stoddard BL (2005) Homing endonuclease structure and function. *Q Rev Biophys* 38: 49–95

Unterweger D, Kostiuk B, Ötjengerdes R, Wilton A, Diaz-Satizabal L & Pukatzki S (2015) Chimeric adaptor proteins translocate diverse type VI secretion system effectors in Vibrio cholerae. *EMBO J* 34: 2198–210

Vettiger A & Basler M (2016) Type VI Secretion System Substrates Are Transferred and Reused among Sister Cells. *Cell* 167: 99-110.e12

Whitney JC, Peterson SB, Kim J, Pazos M, Verster AJ, Radey MC, Kulasekara HD, Ching MQ, Bullen NP, Bryant D, *et al* (2017) A broadly distributed toxin family mediates contact-dependent antagonism between gram-positive bacteria. *Elife* 6: e26938

Zhang D, de Souza RF, Anantharaman V, Iyer LM & Aravind L (2012) Polymorphic toxin systems: Comprehensive characterization of trafficking modes, processing, mechanisms of action, immunity and ecology using comparative genomics. *Biol Direct* 7: 18

Zimmermann L, Stephens A, Nam S-Z, Rau D, Kübler J, Lozajic M, Gabler F, Söding J, Lupas AN & Alva V (2018) A Completely Reimplemented MPI Bioinformatics Toolkit with a New HHpred Server at its Core. *J Mol Biol* 430: 2237–2243